Desalination and Water Treatment
www.deswater.com
doi: 10.5004/dwt.2022.29114

280 (2022) 177–187
December

Adsorption process for removing hazardous Congo red dye from aqueous solutions: isotherm, kinetic, and thermodynamic studies

Hadi S. Al-Lami[a,*], Ali A. Abdulwahid[a], Alaa A. Mizhir[b]

[a]*Department of Chemistry, College of Science, University of Basrah, Basrah, Iraq, Tel. +964 770 737 7488; emails: hadi.abbas@uobasrah.edu.iq (H.S. Al-Lami), Tel. +964 780 140 0141; email: alirazaq2013@yahoo.com (A.A. Abdulwahid)*
[b]*Department of Applied Marine Science, Faculty of Marine Science, University of Basrah, Basrah, Iraq, Tel. +964 782 532 0622; email: allbahily79@yahoo.com*

Received 13 May 2022; Accepted 3 November 2022

ABSTRACT

The removal of Congo red dye from aqueous solutions by adsorption reaction onto three distinct adsorbents: graphene oxide (GO), graphene oxide-grafted-3,3′-diaminobenzidine (GO/DAB), and GO/DAB-grafted-ethylenediaminetetraacetic acid (GO/DAB/EDTA) was investigated in batch experiments. The study of the effects of pH and contacting time on adsorption systems is the first step in optimizing them. The results revealed that depending on the type of adsorbent, the optimum pH values and periods differed. The Congo red (CR) dye adsorptions onto the investigated adsorbents GO, GO/DAB, and GO/DAB/EDTA required pH (3.0, 7.0, and 5.0, respectively) and time (60, 30, and 45 min). The fundamental adsorption properties of the dye were evaluated using adsorption equilibrium isotherms, namely the Langmuir, Freundlich, and Dubinin–Radushkevich models. The maximum adsorption values (q_{max}) were calculated using the Langmuir isotherm results, and they were 1,250; 1,428.5 and 1,438.1 mg/g for the adsorption of CR dye onto adsorbents GO, GO/DAB, and GO/DAB/EDTA, respectively, and these results proved the preference for prepared GO-derivatives over GO. The kinetic models, namely pseudo-first-order and pseudo-second-order, were employed to understand the mechanism of the adsorption process, and they fitted very well with the pseudo-second-order kinetic model, which relies on the assumption that chemisorption may be the rate-limiting step. This study reveals that the presence of functional groups and active sites on the studied adsorbent contributed to its high affinity for CR dye adsorption. As a result, they can be used as efficient and cost-effective dye adsorbents in industrial effluent. Thermodynamic parameters including enthalpy $\Delta H°$, entropy $\Delta S°$, free energy $\Delta G°$, and activation energy E_a of the adsorption process were calculated and used to interpret the results, which revealed that the adsorption systems were a spontaneous and endothermic process for GO and its composites. Also, low activation energy values (E_a < 40 kJ/mol) were characteristics of the physisorption mechanism and diffusion-controlled process.

Keywords: Congo red; Adsorption; Hazardous; Isotherm; Desorption; Pseudo-second-order; Activation energy

1. Introduction

Water is the natural and preferred basin for pollutants, and its pollution has become a major public health hazard. If certain elements or conditions are present to the point where the water cannot be used for a given purpose, the water is said to be polluted. Water pollution, according to Olaniran, is defined as the presence of excessive concentrations of dangerous pollutants in water that make it unhealthy

* Corresponding author.

for drinking, bathing, cooking, or other purposes [1]. Water pollution is almost entirely caused by population growth and industrialization, with heavy metal compounds used in industries such as electroplating, cement, metal processing, wood preservatives, paint and pigments, and steel fabrication. These industries generate a significant amount of toxic waste [2,3].

Colored organic compounds, for example, make up a small percentage of the organic components of trash, but their hue makes them unattractive. The presence of phenolic substances such as tannins or lignin (2%–3%), organic colorants (3%–4%), and especially dyes and dye intermediates, causes the color of waste effluents [4].

Chemical pollutants in industrial waste include colored organic dyes, which generally represent a minor fraction of the organic components of waste. Approximately 30% of colors used in industrial processes end up in wastewater [5]. The biggest suppliers of industrial waste are dying industries such as paper, rubber, plastic, food, leather, and textiles. One of the most important environmental concerns is the wastewater produced by these sectors, which has high salinity, high chemical oxygen demand (COD) concentrations, high temperature, high pH (2–12) variation, and strong color, with many of the wastes being toxic and carcinogenic [6].

Even at low concentrations, the presence of dyes in water inhibits oxygen and light penetration, putting the ecosystem at risk due to the impact on biological cycles and photosynthetic activities. They also have negative health consequences, such as jaundice, skin irritation, allergies, heart abnormalities, and mutations [7]. Dyes' synthetic nature and complex aromatic components make them resistant to biological breakdown. As a result, organic dyes are persistent in a variety of environments, and biological processes are unable to entirely remove the colors [8]. They can build up in living tissues, resulting in a variety of illnesses and ailments. As a result, they must be removed from wastewater before its release into the environment [9]. Textile effluents also make up a significant portion of industrial wastewater. Color is released into the environment by untreated wastewater, posing serious harm to freshwater sources, aquatic life, and humans [10].

Traditional methods for removing contaminants include precipitation, membrane filtration, adsorption, and ion exchange [11]. Furthermore, dye removal from contaminated water and industrial waste has been accomplished using a variety of chemical, physical, and biological approaches [12]. Many researchers prefer the adsorption technique to other approaches, and it is commonly employed in wastewater treatment. Most contaminants like dyes and metal ions have been removed from aqueous solutions using adsorbents such as clay minerals, oxides, graphene, and graphene oxide [13–15].

The adsorption process occupies an important position in environmental remediation [16], and it is a removal process where certain molecules are bound to a particle surface by either chemical or physical attraction [17]. For example, the environmental applications of graphene oxide and its derivatives as adsorbents have recently been investigated, and these materials have demonstrated outstanding adsorption capabilities against a variety of dangerous compounds in an aqueous solution [18]. The composite of polyaniline and reduced graphene oxide (PANI/rGO) was used as the effective adsorbent for the adsorption of mercury(II) in aqueous solutions compared to PANI [19]. Based on the synergy effect, polypyrrole (PPy)/graphene oxide (GO) composite nanosheets exhibited enhanced properties for Cr(VI) ion removal in an aqueous solution [20].

The goal of this study was to modify GO to prepare graphene oxide-grafted-3,3′-diaminobenzidine (GO/DAB) and GO/DAB-grafted-ethylenediaminetetraacetic acid (GO/DAB/EDTA) to increase functional groups which are responsible for the adsorption of a toxic Congo red dye from wastewater and compare it with the base material graphene oxide (GO). The current research will also look at the dye's adsorption mechanisms onto the modified GO (i.e., GO/DAB and GO/DAB/EDTA) surfaces in terms of thermodynamics and kinetics, as well as the many physicochemical parameters that influence the rate of adsorption and the adsorbent's capacity. The Langmuir, Freundlich, and Dubinin–Radushkevich isotherms will be used to characterize the adsorption isotherms. Finally, desorption research is necessary to determine the reusability of the used adsorbents as well as to comprehend the nature of the adsorption system and assess its recycling potential.

2. Experimental

2.1. Materials and measurements

The adsorbents employed in this work are graphene oxide (GO), graphene oxide-grafted-3,3′-diaminobenzidine (GO/DAB), and graphene oxide/DAB-grafted-ethylene diaminetetraacetic acid (GO/DAB/EDTA). They were prepared and characterized as described in our previous published work [15,16].

The anionic diazo Congo red (CR) dye (pH_{zpc} equal to 7), concentrated sulfuric acid (H_2SO_4), sodium chlorate ($NaClO_4$), hydrochloric acid (HCl, 36%), and sodium hydroxide (NaOH) were all provided by Sigma-Aldrich Company. All of the solutions were prepared with distilled or double-distilled water.

A UV-Visible spectrophotometer model T180 was used to detect changes in CR dye concentration before and after the adsorption process in a quartz cell 1 cm long with a maximum wavelength of 494 nm.

2.2. Preparation of an aqueous dye solution

A Congo red dye with FW = 696.7 and a maximum wavelength of 497 nm was used. The 1,000 mg/L stock solution was made for the adsorption investigations, and the required concentrations were obtained by diluting with double deionized water.

2.3. Optimization of adsorption experiments

2.3.1. Initial concentration of CR dye

Different concentrations of Congo red dye were prepared to get the best starting concentration: 100, 200, 300, 400, and 500 mg/L. For each amount of beginning concentration, a fixed 0.025 g of adsorbent was used with 0.1 L of dye solution for 24 h at 27°C.

2.3.2. Acid function pH

The effect of pH on the CR dye adsorption was studied at an initial concentration of 300.0 mg/L of adsorbents GO, GO/DAB, and GO/DAB/EDTA. 0.025 g as a fixed weight of tested adsorbents was used with 0.1 L of CR solutions for 24 h at 27°C. The pH adjustment of the CR dye solution was accomplished by using 0.10 M of hydrochloric acid or sodium hydroxide solution for the range 2–12. The equilibrium concentration of the remaining CR dye was then determined.

2.3.3. Determination of contact time for CR dye

A 0.1 L of 300.0 mg/L CR starting concentration of adsorbents GO, GO/DAB, and GO/DAB/EDTA was applied to a set of 0.025 g as a known amount of adsorbents to determine the equilibrium period of the adsorption investigation. At room temperature, all solutions were shaken at 200 rpm for 1, 3, 9, 12, 15, 30, 45, 60, 75, and 90 min. The equilibrium concentration of reaming CR dye was determined with a UV-Visible Spectrophotometer at λ_{max} = 494 nm, and the optimum pH was 3.0 for GO, 5.0 for GO/DAB/EDTA, and 7.0 for GO/DAB.

2.3.4. Temperature

Three temperature degrees, 27°C, 40°C, and 60°C, were chosen to investigate the effect of temperature on the adsorption process using 300 mg/L. This approach is well known for providing good conditions for the adsorption process.

2.4. Adsorption isotherm

Batch adsorption studies with GO, GO/DAB, and GO/DAB/EDTA were used to determine the adsorption isotherms for CR dye at concentrations of 300, 325, 350, 375, 400, and 450 mg/L at 27°C, and the remaining CR dye concentration was then measured.

2.5. Adsorption kinetics

Adsorption kinetics and calculating thermodynamic parameters such as standard enthalpy change $\Delta H°$, standard entropy change $\Delta S°$, and standard free energy change $\Delta G°$ of CR dye were studied. The experiments were conducted at the chosen temperatures in this study: 27°C, 40°C, and 60°C, with a fixed 0.025 g of adsorbents in 0.1 L of CR dye solution with an initial concentration of 300.0 mg/L for GO, GO/DAB, and GO/DAB/EDTA. The maximum adsorption capacities were found at optimum pH; 3.0 for GO; 5.0 for GO/DAB/EDTA; and 7.0 for GO/DAB with shaking of 200 rpm. Finally, the solution was filtrated and the concentration was determined by a UV-Visible Spectrophotometer at λ_{max} = 494 nm.

2.6. Desorption studies

Several rounds of adsorption/desorption tests utilizing the same adsorbents were utilized to desorb the CR from the currently used adsorbents. In this investigation, maximal dye adsorption was achieved by using the best agitation time and pH value for each adsorbent. The dye-loaded adsorbents were immersed in 100.0 mL of distilled water as the eluent for the desorption studies, and the mixture was stirred continuously at room temperature at the worst pH of each system. At the maximum concentration of each dye, the desorbed dyes were filtered and their concentration was evaluated using a UV-Visible Spectrophotometer.

3. Results and discussion

3.1. Batch adsorption experiments

The batch system was employed in adsorption experiments of CR dye onto prepared adsorbents at optimum pH, contact time, temperature, and the initial concentration (C_o). The amount of the CR adsorbed on each adsorbent used was calculated from the difference in dye concentration in the aqueous phase before and after adsorption, using Eq. (1) [21]:

$$\frac{C_e}{q_e} = \frac{1}{\left(q_{max} K_L\right)} + \frac{C_e}{q_{max}} \tag{1}$$

where C_o and C_e (mg/L) are the initial and equilibrium dye concentrations in the solution, V (L) is the dye solution volume, m (g) is the mass of the employed adsorbents in the experiment, and q_e (mg/g) is the amount of adsorbed dyes per gram of adsorbents (adsorption capacity).

3.1.1. Effect of pH on the CR

The solution chemistry of dyes, complexation by organic or inorganic ligands, precipitation, and hydrolysis are all influenced by pH. The speciation and availability of dyes for adsorption are similarly influenced by pH [22]. At an ideal initial CR dye concentration, the effect of pH on the adsorption capabilities of evaluated adsorbents was investigated. The pH influence was changed at the range (3.0–12.0) of the adsorption capabilities for CR dye onto GO, GO/DAB, and GO/DAB/EDTA at 27°C, as shown in Fig. 1.

Fig. 1 shows a sharp decrease in the adsorption of CR dye with increasing pH from 3.0 to 7.0. A lower q_{max} is found for GO adsorbents at pH ranging from 9.0 to 12.0. However, the optimum pH for adsorption depends on the types of adsorbate and adsorbent. It was found that the best working pH value is 7.0 for the better adsorption of CR dye by GO/DAB, with a sharp increase when the pH increases from 3.0 to 7.0, while lower adsorption capacity is obtained in the pH range from 9.0 to 12.0 for the same adsorbent. As a result, the pH was maintained at 7.0 in subsequent tests, and these results are in good agreement with results reported for the elimination of CR dye by sorption over aniline propyl silica aerogel [23], and it may be directly related to the pH_{zpc} of CR, which is equal to 7 at the neutral pH where the electrostatic interactions are less than in acidic or basic media.

Similar behavior is observed for CR dye adsorption onto GO/DAB/EDTA adsorbents. Adsorption depends on the extent of protonation of the carboxylic groups in the graphene oxide and carboxyl and carbonyl groups in the

EDTA [24]. Fig. 1 also shows that the adsorption efficiency is lower in acidic media (pH 3.0) for GO/DAB/EDTA, and there is an increase in CR dye adsorption when the pH value is increased from 3.0 to 5.0. Therefore, pH 5.0 is optimized for the adsorption of CR dye onto GO/DAB/EDTA. After that, the lower adsorption capacity is found at a pH range of 7.0 to 12.0, also for the adsorbent GO/DAB/EDTA.

The adsorption process is dependent on the pH of the solution since it affects the adsorbent surface charge and the degree of protonation of the functional groups [22]. With increasing pH values, the adsorption of CR dye on GO tends to decrease due to the rising electrostatic repulsion between the anionic dye adsorbate species and negatively charged adsorbent surfaces. In addition, lower adsorption at alkaline pH is due to the presence of excess OH ions, which destabilize anionic dye and compete with the dye anions for the adsorption sites. Low pH leads to an increase in H^+ ion concentration in the system. By absorbing H^+ ions, the surface of adsorbents gains a positive charge, allowing for increased anionic dye adsorption. The adsorption of CR dye on agricultural stable waste-based activated carbon showed similar behavior [25].

3.1.2. Effect of contact time and temperatures

The agitation time is the amount of time it takes for the adsorption process to reach equilibrium. As a result, the contact time between the adsorbate and the adsorbent is critical in the adsorption process, and the time required to reach equilibrium is crucial in predicting the performance and practicality of an adsorbent for a given procedure [26].

At the initial concentration and optimum pH, the effect of agitation time on the adsorption of CR dye onto the tested adsorbents GO, GO/DAB, and GO/DAB/EDTA is shown in Figs. 2–4, respectively, at three different temperatures: 27°C, 40°C, and 60°C.

It can be noted from Figs. 2–4 that the adsorption capacity increased as it reached equilibrium for all adsorbents. Therefore, the optimum agitation time was chosen at the point of equilibrium, which was 60, 30, and 45min for the adsorption of CR dye onto GO, GO/DAB, and GO/DAB/EDTA, respectively.

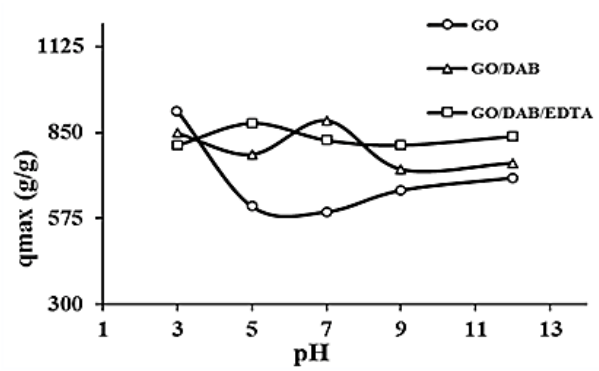

Fig. 1. Effect of pH on the adsorption of Congo red CR onto adsorbents at 27°C.

3.2. Isotherm of CR adsorption

The adsorption isotherm shows the distribution of molecules between solid and liquid phases at an equilibrium state. The analysis of isotherm data by fitting them to different isotherm models is an essential step in finding the most suitable model that can be used to describe the adsorption

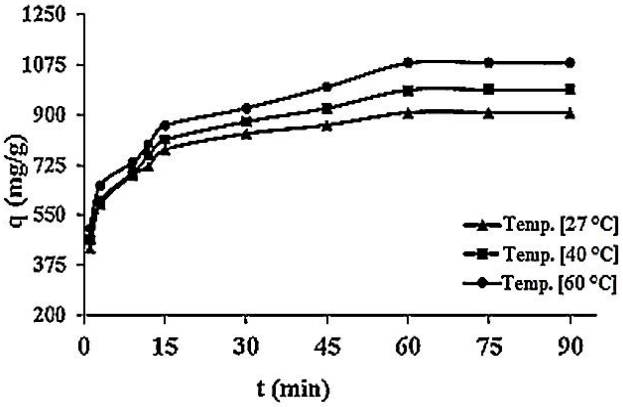

Fig. 2. Agitation time effect of the CR dye adsorption onto GO at different temperatures.

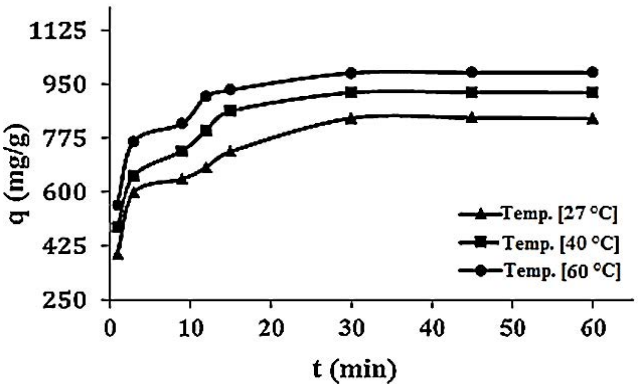

Fig. 3. Agitation time effect of the CR dye adsorption onto GO/DAB at different temperatures

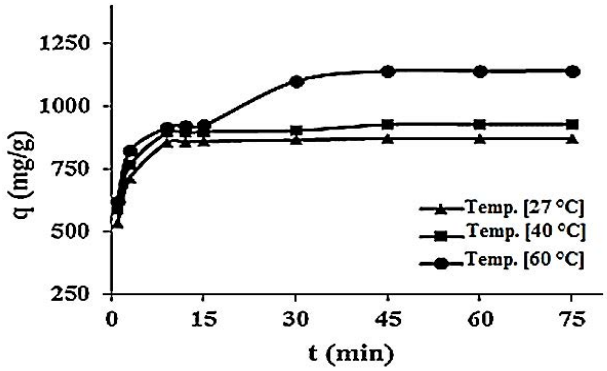

Fig. 4. Influence of agitation time on CR dye adsorption onto GO/DAB/EDTA at various temperatures.

process [27]. For analyzing the experimental adsorption results, there are several isotherm models to describe the isotherm data. In this study, Langmuir, Freundlich, Temkin, and Dubinin–Radushkevich models are employed.

3.2.1. Langmuir isotherm

The Langmuir model depends upon the maximum adsorption that coincides with the saturated monolayer of adsorbate (liquid molecules) on the adsorbent (solid surface). The Langmuir equation is valid for monolayer adsorption of the adsorbate onto the surface of the adsorbent and assumes there are restricted and homogenous adsorption sites. The linearized form of the Langmuir model is given as follows [28].

$$\frac{C_e}{q_e} = \frac{1}{\left(q_{\max} K_L\right)} + \frac{C_e}{q_{\max}} \tag{2}$$

where C_e (mg/L) is the dye equilibrium concentration; $q_{\max}$ (mg/g) is the adsorption capacity required to complete a monolayer on the adsorbent surface; q_e (mg/g) is the amount of adsorbate per unit mass of adsorbent at equilibrium, and k_L (L/mg) is the Langmuir constant that relates to the energy of the adsorption process. The slope of plotting C_e/q_e vs. C_e is equal to $(1/q_{\max})$ and the intercept is equal to $(1/q_{\max}\cdot k_L)$.

Erdem et al. [29] reported that the essential characteristics of a Langmuir isotherm could be expressed in terms of a dimensionless constant separation factor or equilibrium parameter R_L, which is defined by:

$$R_L = \frac{1}{1+\left(K_L.C_e\right)} \tag{3}$$

where R_L is indicative of the isotherm shape and predicts whether a sorption system will be either favorable ($0 < R_L < 1$), unfavorable ($R_L > 1$), or irreversible ($R_L = 0$). Fig. 5 gives the plots of the Langmuir isotherms of CR dye adsorbed onto GO, GO/DAB, and GO/DAB/EDTA, respectively, and Table 1 displays $q_{\max}$, k_L, R_L, and the correlation coefficient R^2 results for the Langmuir isotherms for the adsorption of the dye CR by the tested adsorbents.

The obtained correlation coefficients R^2 for the Langmuir (as shown in Table 1) are $1 \geq R^2 \geq 0.9969$ for CR dye. This describes the participation of the chemisorption mechanism in the adsorption process of dyes on the prepared adsorbents. In addition, to determine whether the adsorption process is favorable or unfavorable for the Langmuir isotherm model, the values of constant separation factor R_L, defined in Eq. (3), are all between one and zero, implying the presence of a favorable condition for the adsorption process of the tested adsorbents by CR dye ($0.0316 \leq R_L \leq 0.6063$). Besides that, the R_L values of the adsorbents shown in Table 1 are lower than those of graphene oxide, which indicates these tested adsorbents from GO have a higher affinity toward CR dye.

This also indicates the formation of a monolayer of adsorbate molecules onto the homogeneous surface of the tested adsorbent. It could be said there was a tendency for chemical adsorption to exist between functional groups of prepared adsorbents and dyes [30]. The results also show that the $q_{\max}$ of the prepared adsorbents has values higher than graphene oxide. This implies that these adsorbents have the capacity and efficiency to absorb the CR dye from their aqueous solutions.

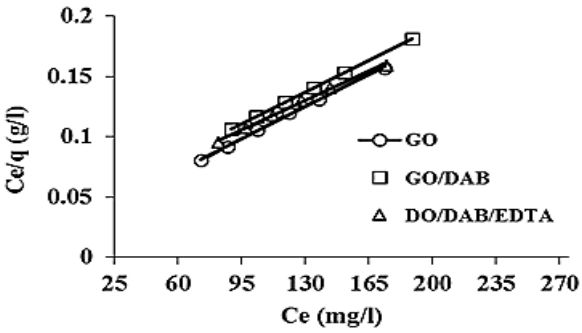

Fig. 5. Langmuir adsorption isotherm of CR dye onto adsorbents at 27°C.

Table 1
Isotherms parameters for the adsorption of CR dye onto adsorbents at 27°C

Langmuir isotherm parameters				
Adsorbent	$q_{\max}$ (L/mg)	k_L (L/mg)	R_L	R^2
GO	1,250.0	0.0312	0.6063	0.9987
GO/DAB	1,428.5	0.0177	0.1579	1.0
GO/DAB/EDTA	1,438.1	0.0178	0.1573	0.9969
Freundlich isotherm parameters				
Adsorbent	k_F (mg/g)		$1/n$	R^2
GO	348.278		0.2236	0.9982
GO/DAB	231.042		0.2892	0.9931
GO/DAB/EDTA	220.478		0.3099	0.9962
D–R isotherm parameters				
Adsorbent	$q_{\max}$ (mg/g)	β (mol²/kJ²)	E (kJ/mol)	R^2
GO	1,118.9	2E-04	50.78	0.9332
GO/DAB	1,093.2	4E-04	35.35	0.9798
GO/DAB/EDTA	1,132.6	3E-04	40.82	0.9284

3.2.2. Freundlich isotherm

The Freundlich isotherm model is based on a heterogeneous exponentially decaying distribution, which fits well with the tail portion of the heterogeneous distribution of adsorbent [31]. The general Freundlich isotherm empirical equation is given by:

$$\ln q_e = \ln K_F + \frac{1}{n}\ln C_e \tag{4}$$

where k_F (mg/g) is a constant for the adsorption or distribution coefficient and represents the amount of dye adsorbed onto adsorbents at the equilibrium concentration, and $1/n$ is the empirical parameter correlated to the intensity of the adsorption process or the surface heterogeneity of the adsorbent. A favorable adsorption process occurs with values between zero and one.

Fig. 6 represents the plots of the Freundlich adsorption isotherms of CR dye adsorbed onto GO, GO/DAB, and GO/DAB/EDTA, and Table 1 list k_F, $1/n$, and the correlation coefficient R^2 is determined from the linear plot of $\ln q_e$ vs. $\ln C_e$.

The Freundlich isotherm considers the heterogeneous surface of the adsorbents, and the results indicate that the Freundlich model fits the experimental data less than the Langmuir model since the R^2 values are $0.9931 \le R^2 \le 0.9993$ for CR dye, respectively, as shown in Table 1. Nevertheless, these coefficient correlation values show good linearity.

In addition, the results showed that k_F ranged from 220.478 to 1,006.67 mg/g for CR, while $1/n$ values ranged from 0.1380 to 0.7020, as shown in Table 1, which reflects the strength and practicality of the adsorption process. The CR dye adsorption on adsorbents is less than one, indicating good CR dye adsorption on adsorbents, and it becomes more heterogeneous as it approaches zero in the current investigation [32,33].

3.2.3. Dubinin–Radushkevich isotherm

The Dubinin–Radushkevich (D–R) isotherm is an empirical model initially conceived for the adsorption of subcritical vapors onto micropore solids following a pore-filling mechanism. This is generally applied to express the adsorption mechanism [33]. Even though it has a similar approach to the Langmuir isotherm by rejecting the homogenous surface or constant adsorption potential, the D–R version is more general than the Langmuir version in exploring adsorption isotherms, and the D–R isotherm model equation can be linearized into the following equation [34]:

$$\ln q_e = \ln q_{\max} - \beta\varepsilon^2 \tag{5}$$

where $q_{\max}$ (mg/g) is the D–R monolayer capacity, β (mol²/kJ²) is a constant related to adsorption energy, and ε is the Polanyi potential that is associated with the equilibrium concentration as shown in the equation [35].

$$\varepsilon = RT\ln\left(1+\frac{1}{C_e}\right) \tag{6}$$

where R (kJ/mol·K) is the universal gas constant, T is the temperature in Kelvin, and C_e (mg/L) is the equilibrium concentration of adsorbate in solution. A plot of the amount of the tested adsorbents in the form of $\ln q_e$ vs. ε^2 is shown in Fig. 7 for the adsorption of CR onto GO, GO/DAB, and GO/DAB/EDTA adsorbents.

The constants, such as $q_{\max}$ and, β were determined from the intercept and the slope, respectively. This approach is usually applied to distinguish between the physical and chemical adsorption processes [36]. The mean free energy E per molecule of adsorbate (for removing a molecule from its location in the sorption space to infinity) can be computed by the relationship [37]:

$$E = \frac{1}{\sqrt{2\beta}} \tag{7}$$

From the linear plot of the D–R isotherm model, $q_{\max}$, β (mol²/kJ²), E is the mean free energy of the D–R isotherm (kJ/mol), and R^2 are determined and listed in Table 1 for the adsorption of CR dye by the prepared GO, GO/DAB, and GO/DAB/EDTA adsorbents.

The adsorption behavior could have predicted physical adsorption in the 1–8 kJ/mol range of the mean adsorption energy and chemical adsorption above (8 kJ/mol) of the mean adsorption energy E [17–38]. As shown in Table 1, the values of the mean adsorption energies E calculated using Eq. (7) of the adsorption of CR dye onto GO, GO/DAB, and GO/DAB/EDTA adsorbents are 35.35–168.1, indicating that the adsorptions of CR dye onto these adsorbents were predominant in the chemisorption process [39,40].

Based on the linear plot obtained from the D–R isotherm model and as shown in Table 1, the $q_{\max}$ values are close to the maximum monolayer coverage capacity $q_{\max}$, which is calculated by the Langmuir isotherm model as listed in Table 1.

3.3. Adsorption kinetics

Kinetics data helps to depict dye uptake rates, which control the residence time of adsorbate at the solid-liquid interface and give valuable information for adsorption process design [41]. In addition, the experimental kinetic curves can be assessed using many different models [16–42]. Therefore, in this study, the appropriateness of pseudo-first-order and pseudo-second-order is tested to interpret the mechanism of CR dye adsorption onto the tested adsorbents GO, GO/DAB, and GO/DAB/EDTA.

The first model was pseudo-first-order and is one of the most widely used equations for the sorption of solute from a liquid solution [43], and the mathematical expression of this model is given by Eq. (8):

$$\ln q_e - q_t = \ln q - k_1 t \tag{8}$$

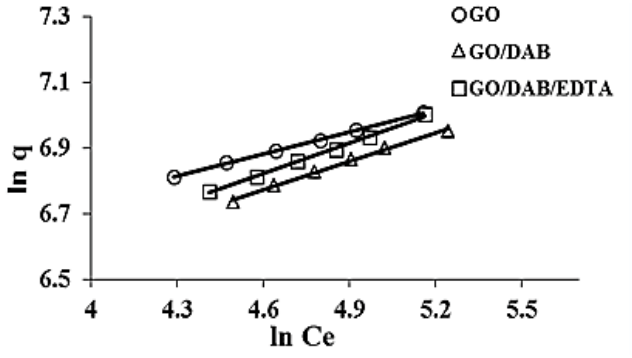

Fig. 6. Freundlich adsorption isotherm of CR dye onto adsorbents at 27°C.

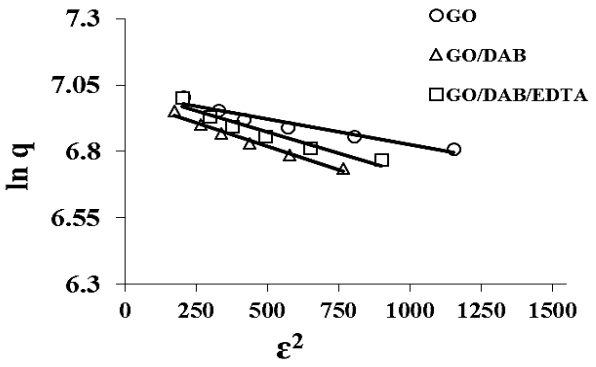

Fig. 7. D–R adsorption isotherm of CR dye onto adsorbents at 27°C.

where q_t and q_1 (mg/g) are the amounts of dye adsorbed at time t and the maximum adsorption capacity for the pseudo-first-order, respectively. k_1 (min^{-1}) is the pseudo-first-order rate constant for adsorption. A plot of ($\ln q_e - q_t$) against (t) will result in a straight line with the slope of k_1 and an intercept of $\ln q_e$. Table 2 lists the values of k_1, q_1, and R^2 of pseudo-first-order parameters obtained from Eq. (8) at different temperatures (27°C, 40°C, and 60°C).

The second kinetic model was pseudo-second-order, which shows the rate based on the sorption equilibrium capacity of the adsorbent and not on the concentration of the adsorbate [44]. This can be represented by Eq. (9):

$$\frac{t}{q_t} = \frac{1}{k_2 q_2^2} + \frac{t}{q_2} \tag{9}$$

where q_2 (mg/g) is the maximum adsorption capacity for the pseudo-second-order and k_2 (g/mg·min) is the equilibrium rate constant for pseudo-second-order adsorption. Values of q_2 and k_2 are calculated from the plotting of (t/q_t) against (t) from the slope and intercept, and the values obtained are listed in Table 2 as well.

The expression of kinetic adsorption models [45] can be used to define the rate-limiting steps in the adsorption process. The pseudo-first-order kinetic model, the most widely used model in the literature, was applied to analyze the dye's adsorption data [46]. Diffusion steps are assumed to be involved in rate-controlling for dye removal from the solution in this model.

The obtained correlation coefficients R^2 for these kinetic adsorption models are ≤0.9969, indicating that the data obtained from the study at different time intervals does not fit the rate equation better than the second-order rate equation [47], as we will notice in Table 2.

The pseudo-first and pseudo-second models are compared for their fitness for dye adsorption by adsorbents. Accepted kinetic models for the adsorption process can be characterized by common validity tests:

- A high correlation coefficient, R^2, indicates that a given kinetic model is applicable and reliable;
- There is a close agreement between the calculated and experimental equilibrium capacity values.

As shown in Table 2, the pseudo-first-order kinetics model's low correlation coefficients, such as (R^2 = 0.7570 and 0.8670 at 40°C) for CR dye onto GO/DAB/EDTA, as well as the lack of match between calculated and experimental q_{max} values of adsorbents toward CR dye, led to the conclusion that this kinetic model did not explain the adsorption process.

The high correlation coefficients ($0.9955 \le R^2 \le 1.0$) as shown in Table 2 and the close match in the values of calculated and experimental q_{max} when applying the pseudo-second-order kinetics model imply the fitting of this model for the CR dye adsorption system. The rate constants k_2 of the adsorption processes for CR did not always increase with increasing temperature, and similar findings between rate constants and temperature were reported in the literature [48,49]. These facts suggest that the adsorption of CR dye by the tested adsorbents favorably relies on the assumption of a chemisorption process [50,51]. The D–R isotherm model also proves the fitting of a pseudo-second-order kinetic model, indicating that the adsorption systems obeyed the chemisorption mechanism.

3.4. Adsorption thermodynamic

Investigating thermodynamic functions such as the change in standard enthalpy $\Delta H°$, change in standard

Table 2
Pseudo-first-order and pseudo-second-order parameters for adsorption of CR dye onto tested adsorbents at different temperatures

Adsorbents	Temp. (°C)	Pseudo-first-order			Pseudo-second-order		
		k_1 (min^{-1})	q_1 (mg/g)	R_1^2	k_2 (g/mg min)	q_1 (mg/g)	R_1^2
GO	27	0.0432	290.84	0.9711	0.00065	735.17	0.9992
	40	0.0394	364.05	0.9747	0.00063	778.38	0.9993
	60	0.0366	440.58	0.9704	0.00060	816.78	0.9993
GO/DAB	27	0.0629	312.93	0.8962	0.00123	1,335.9	0.9992
	40	0.1187	445.23	0.8928	0.00163	1,430.8	1.0000
	60	0.1216	361.83	0.9039	0.00280	1,550.1	0.9999
GO/DAB/EDTA	27	0.0577	25.818	0.9969	0.00213	611.15	0.9998
	40	0.0179	40.056	0.8670	0.00161	678.62	0.9995
	60	0.0884	623.09	0.9402	0.0004	765.32	0.9979

entropy $\Delta S°$, change in standard free energy $\Delta G°$, and activation energy E_a is necessary to comprehend the principles of adsorption reactions [52]. The thermodynamic adsorption studies were carried out at three distinct temperatures: 300.15, 313.15, and 333.15 K.

The important thermodynamic parameters can be determined from the thermodynamic distribution coefficient (equilibrium constant). k_L values were calculated according to Eq. (10) [53]:

$$\Delta G° = \Delta H° - T\Delta S° \tag{10}$$

where C_a is the equilibrium concentration of dye on the adsorbents (mg/g) and C_e is the concentration of dye in the solution (mg/L). The results of thermodynamic studies make it conceivable to understand the feasibility of the adsorption process and to get helpful data about fundamental parameters of adsorption, such as $\Delta H°$ and $\Delta S°$ that can be calculated using equation 11 [54]:

$$\ln K_L = \frac{\Delta S°}{R} - \frac{\Delta H°}{RT} \tag{11}$$

where R is the universal gas constant (8.314 J/mol·K), and T (K) is the absolute temperature. The calculated values are listed in Table 3.

The standard Gibbs free energy $\Delta G°$ (kJ/mol) values are computed for each temperature used in the study (300.15, 313.15, and 333.15 K) of CR dye adsorption processes from the following Helmholtz relation Eq. (12) [55]:

$$\Delta G° = \Delta H° - T\Delta S° \tag{12}$$

The activation energy E_a (kJ/mol) of the adsorption process represents the minimum energy that reactants must have for the reaction to proceed, and it was calculated from the Arrhenius equation, as shown by the following relationship [56]:

$$\ln K = \ln A - \frac{E_a}{RT} \tag{13}$$

where K (g/mg·min) is the rate constant obtained from the pseudo-second-order kinetic model in an adsorption system of CR dye for all prepared adsorbents, and A is the Arrhenius factor. The values of the thermodynamic parameters in our current study; $\Delta H°$, $\Delta S°$, $\Delta G°$, and E_a calculated from the equations, are listed in Table 4 for the adsorption of CR dye onto the prepared adsorbents GO, GO/DAB, and GO/DAB/EDTA.

All parameters shown in Table 3 are the actual indicators for practical applications of the dye adsorption process. $\Delta G°$ indicates whether the reaction is spontaneous or non-spontaneous, $\Delta H°$ determines whether the dye adsorption process is exothermic or endothermic, and $\Delta S°$ indicates the degree of disorder at the solid-liquid interface during the dye adsorption process.

The calculated thermodynamic parameters showed the positive values of enthalpy changes $\Delta H°$ for the adsorption of CR dye onto prepared adsorbents GO, GO/DAB, and GO/DAB/EDTA, indicating that the adsorption processes were endothermic. The positive value of entropy $\Delta S°$ suggests an increase in the randomness at the (adsorbents/solution) interface and an affinity towards the dye [56]. This is because of the increase in mobility of adsorbate ions present in the solution while raising the temperature. The negative values of $\Delta G°$ (as shown in Table 3) reveal that the adsorption process on the prepared adsorbents is a spontaneous reaction at any temperature. This implies that the adsorption system does not require an external energy source.

The low values of activation energy (E_a < 40 kJ/mol) for all the prepared adsorbents are characteristics of the physisorption and diffusion-controlled processes [57], showing that the adsorption process of CR dye (E_a CR = −78.010 to 13.693 kJ/mol) by the prepared adsorbents is governed by a physisorption mechanism involving Van der Waals forces between the charged sites of the dyes and the surface of the adsorbents. Therefore, these results indicate that the adsorption processes of CR dye onto adsorbents are diffusion-controlled and physical.

The calculated $\Delta G°$ between (−1.856 and −7.734) kJ/mol suggested that the adsorption of CR dye on the prepared adsorbents could be regarded as a physical adsorption process at the studied temperatures. The $\Delta G°$ for physisorption was reported to be in the range of 20 to 0 kJ/mol, physisorption plus chemisorption between 80 and 20 kJ/mol, and chemisorption within 400 to 80 kJ/mol [58].

As a result, the adsorption process gives an impression of chemical and physical behavior, where the adsorption process might be chemisorption as shown previously in the isotherm study (Langmuir and D–R), and physisorption through the thermodynamic study. Therefore, this means that the adsorption process of CR dye onto adsorbents was a physiochemical adsorption approach.

3.5. Desorption experiment of CR

It was important to renew both adsorbents and dyes, which could be recycled again, to make the adsorption process more cost-effective [59]. Understanding the adsorption mechanism of adsorbate onto an adsorbent necessitates desorption process research. The purpose of desorption is to remove reversible adsorbate molecules

Table 3
Thermodynamic parameters for adsorption of CR dye onto prepared adsorbents at different temperatures

Adsorbent	Temp.	$\Delta H°$	$\Delta S°$	$-\Delta G°$	E_a
	300.15			2.782	
GO	313.15	27.462	100.766	4.092	13.963
	333.15			6.107	
	300.15			2.193	
GO/DAB	313.15	17.052	64.118	3.026	–11.642
	333.15			4.309	
	300.15			1.856	
GO/DAB/EDTA	313.15	51.600	178.103	4.172	–78.013
	333.15			7.734	

from the adsorbent and replenish the adsorbents [60]. The efficiency of the dyes' desorption removal (%*S*) was calculated by Eq. (14) [61]:

$$S = \frac{C_d V_d}{q_e W} \times 100\% \quad (14)$$

where q_e (mg/g) is the equilibrium amount of dye adsorbed on the adsorbent, C_d (mg/L) is the dye concentration in solution after desorption, and V_d (mL) is the volume of the eluent (desorbing reagent).

Table 4 shows the adsorption–desorption process of CR dye from the tested adsorbents using distilled water as adsorption agent for three cycles. The decrease in adsorption efficiency from cycle one to cycle three was (31.13%, 32.45%, 29.51%, 34.25%, 34.12%, and 37.07%) was adsorbed by GO, GO/DAB, and GO/DAB/EDTA, respectively. This implies that these adsorbents could be used several times while retaining their good adsorption capacity, and a relatively low percentage of the desorption values (%*S*) suggests that both dyes were chemisorbed onto the surface of GO-modified adsorbents compared to graphene oxide [62].

A desorption study gives a good explanation of the significant characteristics of an appropriate adsorbent for practical applications. Besides, the regeneration of adsorbents generally leads to the recovery of dyes, reuse of adsorbents in the adsorption study, and a lower cost of the adsorption process [63].

The desorption percentages (%*S*) obtained for GO were (81.32%, 70.33%, and 62.11%) for the three cycles run, and these desorption percentages were higher than those of the other two adsorbents derived from GO, that is, GO/DAB and GO/DAB/EDTA. This may be attributed to the sufficient functional groups in these derivatives (the adsorption sites) compared with GO, which led to a better understanding of the role of functional groups in these adsorbents under study.

Table 4
Adsorption/desorption for CR dye onto tested adsorbents

Cycle No.	GO		GO/DAB		GO/DAB/EDTA	
	q_e (mg/g)	%*S*	q_e (mg/g)	%*S*	q_e	%*S*
1	1,050.31	81.32	1,096.82	68.48	1,168.22	77.03
2	841.66	70.33	863.41	55.93	958.98	68.14
3	723.33	62.11	740.68	44.07	823.74	57.04

3.6. Comparison with some reported methods

The adsorption of Congo red dye onto graphene oxide and its derivatives was considered in the current work. Any study must be evaluated by comparing its findings to those of other studies to ascertain its significance. A comparison between this work and other systems published in the literature [64–67] is shown in Table 5.

4. Conclusions

The results of this study reveal that the GO, GO/DAB, and GO/DAB/EDTA adsorbents can be employed to remove CR dye from aqueous solutions. Langmuir, Freundlich, and Dubinin–Radushkevich described the equilibrium data, and the results fit well with the Langmuir model, showing that the adsorption process is advantageous for monolayer chemisorption coverage. The maximum adsorption values (q_{max}) of CR dye onto the adsorbents GO, GO/DAB, and GO/DAB/EDTA, respectively, were 1,250; 1,428.5 and 1,438.1 mg/g, demonstrating a preference for produced GO-derivatives over GO, and it is heavily influenced by the dye aqueous solution pH and contacting time, which vary depending on the type of adsorbent. In comparison to the reference GO, the GO/DAB and GO/DAB/EDTA adsorbents required various times to reach equilibrium.

Depending on the value of the correlation coefficient R^2, the pseudo-second-order kinetic model accurately reflected the adsorption kinetics of CR dye onto the three adsorbents used. The adsorption capacities of GO, GO/DAB and GO/DAB/EDTA increased as the temperature increased.

The results showed that the adsorption systems were a spontaneous and endothermic process for GO and its composites. The results were interpreted using the thermodynamic characteristics of the adsorption process, including enthalpy, entropy, free energy, and activation energy.

Table 5
Comparison of maximum adsorption capacities of CR onto GO, GO/DAB and GO/DAB/EDTA adsorbents and other adsorbents

Adsorbent	Adsorption capacity (mg/g)	References
Acrylamide, HEMA, N-isopropylacrylamide and perylene-5-ylpent-3-yne-2-methylprop-2-enoate-co-2-methyl-2-(prop-2-enoylamino)propane-1-sulfonic acid (PePnUMA-co-AMPS)	1,666.7	[57]
MgO	18.86	[58]
g-Al_2O_3 nanoshells	370.4	[59]
MgAl-layered double hydroxide (MgAl-LDH) nanosorbents	769.23	[60]
Graphene oxide	1,250.0	This work
Graphene oxide-grafted-3,3′-diaminobenzidine (GO/DAB)	1,428.5	This work
GO/DAB-grafted-ethylenediaminetetraacetic acid (GO/DAB/EDTA)	1,438.1	This work

Both the diffusion-controlled process and the physisorption mechanism exhibited low activation energy levels ($E_a \approx 40$ kJ/mol).

The desorption–adsorption tests demonstrated that the generated adsorbents were reusable and stable after the third cycle. The study could be relevant in a variety of applications needing enhanced industrial wastewater treatment using the evaluated adsorbents, according to the significance of the findings.

Acknowledgment

This paper and the research behind it would not have been possible without the exceptional effort put forth by Mr. Alaa A. Mizhr during his Ph.D. research work.

References

[1] J.U. Kujoh, A.A. Ojong, J.E. Effiom, F.A. Dan, Environmental health education as a tool for environmental protection in Nigeria Universities, Pal. Arch. J. Eyg., 17 (2020) 10462–10468.
[2] S.K. Singh, Water pollution: sources, effects, and control measures, J. Agroe. Nat. Res. Manage., 3 (2016) 64–66.
[3] C. Raji, T.S. Anirudhan, Chromium(VI) adsorption by sawdust carbon: kinetics and equilibrium, Indian J. Chem. Technol., 4 (1997) 228–236.
[4] M.V. Tuttolomondo, G.S. Alvarez, M.F. Desimone, L.E. Diaz, Removal of azo dyes from water by sol–gel immobilized *Pseudomonas* sp., J. Environ. Chem. Eng., 2 (2014) 131–136.
[5] E. Brillas, C.A. Martínez-Huitle, Decontamination of wastewaters containing synthetic organic dyes by electrochemical methods. An updated review, Appl. Catal., B, 166 (2015) 603–643.
[6] D. El-Mekkawi, H. Galal, Removal of a synthetic dye "Direct Fast Blue B2RL" via adsorption and photocatalytic degradation using low-cost rutile and Degussa P25 titanium dioxide, J. Hydro-Environ. Res., 7 (2013) 219–226.
[7] G. Crini, Non-conventional low-cost adsorbents for dye removal: a review, Bioresour. Technol., 97 (2006) 1061–1085.
[8] S.P. Buthelezi, A.O. Olaniran, B. Pillay, Textile dye removal from wastewater effluents using bioflocculants produced by indigenous bacterial isolates, Molecules, 17 (2012) 14260–14274.
[9] W.W. Ngah, M. Hanafiah, Removal of heavy metal ions from wastewater by chemically modified plant wastes as adsorbents: a review, Bioresour. Technol., 99 (2008) 3935–3948.
[10] S. Sathian, M. Rajasimman, G. Radha, V. Shanmugapriya, C. Karthikeyan, Performance of SBR for the treatment of textile dye wastewater: optimization and kinetic studies, Alexandria Eng. J., 53 (2014) 417–426.
[11] M.M. Matlock, B.S. Howerton, D.A. Atwood, Chemical precipitation of lead from lead battery recycling plant wastewater, Ind. Eng. Chem. Res., 41 (2002) 1579–1582.
[12] G. Ratnamala, K. Brajesh, Biosorption of removal navy blue dye from an aqueous solution using *Pseudomonas putida*, Int. J. Sci. Environ. Technol., 2 (2013) 80–89.
[13] B. Fonseca, H. Figueiredo, J. Rodrigues, A. Queiroz, T. Tavares, Mobility of Cr, Pb, Cd, Cu and Zn in a loamy sand soil: a comparative study, Geoderma, 164 (2011) 232–237.
[14] X. Tan, Q. Fan, X. Wang, B. Grambow, Eu(III) sorption to TiO_2 (anatase and rutile): batch, XPS, and EXAFS studies, Environ. Sci. Technol., 43 (2009) 3115–3121.
[15] A.A. Mizhir, A.A. Abdulwahid, H.S. Al-Lami, Chemical functionalization graphene oxide for the adsorption behavior of bismarck brown dye from aqueous solutions, Egypt. J. Chem., 63 (2020) 1679–1696.
[16] A.A. Mizhir, Preparation of Graphene Oxide–Grafted Polymers and the Analytical Study of Their Interaction with Congo red and Bismarck Brown Dyes, Ph.D. Thesis, University of Basrah, Iraq, 2020.
[17] A.A. Mizhir, A.A. Abdulwahid, H.S. Al-Lami, Adsorption of carcinogenic dye Congo red onto prepared graphene oxide-based composites, Desal. Water Treat., 202 (2020) 381–395.
[18] V. Chandra, K.S. Kim, Highly selective adsorption of Hg^{2+} by polypyrrole–reduced graphene oxide composite, Chem. Commun., 47 (2011) 3942–3944.
[19] R. Li, L. Liu, F. Yang, Preparation of polyaniline/reduced graphene oxide nanocomposite and its application in adsorption of aqueous Hg(II), Chem. Eng. J., 229 (2013) 460–468.
[20] L. Yang, Z. Li, G. Nie, Z. Zhang, X. Lu, C. Wang, Fabrication of poly(o-phenylenediamine)/reduced graphene oxide composite nanosheets via microwave heating and their effective adsorption of lead ions, Appl. Surf. Sci., 307 (2014) 601–607.
[21] P. Pauletto, J. Gonçalves, L. Pinto, G. Dotto, N. Salau, Single and competitive dye adsorption onto chitosan-based hybrid hydrogels using artificial neural network modeling, J. Colloid Interface Sci., 560 (2020) 722–729.
[22] R. Han, W. Zou, Z. Zhang, J. Shi, J. Yang, Removal of copper(II) and lead(II) from aqueous solution by manganese oxide coated sand: I. Characterization and kinetic study, J. Hazard. Mater., 137 (2006) 384–395.
[23] F.A. Pavan, S.L. Dias, E.C. Lima, E.V. Benvenutti, Removal of Congo red from aqueous solution by aniline-propyl silica xerogel, Dyes Pigm., 76 (2008) 64–69.
[24] I.E.M. Carpio, J.D. Mangadlao, H.N. Nguyen, R.C. Advincula, D.F. Rodrigues, Graphene oxide functionalized with ethylenediamine tri acetic acid for heavy metal adsorption and anti-microbial applications, Carbon, 77 (2014) 289–301.
[25] C. Namasivayam, D. Kavitha, Removal of Congo red from water by adsorption onto activated carbon prepared from coir pith, an agricultural solid waste, Dyes Pigm., 54 (2002) 47–58.
[26] S. Mishra, D. Mohapatra, D. Mishra, P. Chattopadhyay, G.R. Chaudhury, R. Das, Arsenic adsorption on natural minerals, J. Mater. Environ. Sci., 5 (2014) 350–359.
[27] B. Royer, N.F. Cardoso, E.C. Lima, J.C.P. Vaghetti, N.M. Simon, T. Calvete, R.C. Veses, Applications of Brazilian pine-fruit shell in natural and carbonized forms as adsorbents to removal of methylene blue from aqueous solutions—kinetic and equilibrium study, J. Hazard. Mater., 164 (2009) 1213–1222.
[28] I. Langmuir, The constitution and fundamental properties of solids and liquids. Part I. Solids, J. Am. Chem. Soc., 38 (1916) 2221–2295.
[29] M. Erdem, E. Yüksel, T. Tay, Y. Çimen, H. Türk, Synthesis of novel methacrylate-based adsorbents and their sorptive properties towards p-nitrophenol from aqueous solutions, J. Colloid Interface Sci., 333 (2009) 40–48.
[30] M.-H. Baek, C.O. Ijagbemi, O. Se-Jin, D.-S. Kim, Removal of Malachite green from aqueous solution using degreased coffee bean, J. Hazard. Mater., 176 (2010) 820–828.
[31] H.B. Senturk, D. Ozdes, A. Gundogdu, C. Duran, M. Soylak, Removal of phenol from aqueous solutions by adsorption onto organomodified Tirebolu bentonite: equilibrium, kinetic and thermodynamic study, J. Hazard. Mater., 172 (2009) 353–362.
[32] M.T. Sultan, H.S. Al-Lami, A.H. Al-Dujiali, Synthesis and characterization of alumina-grafted acrylic acid monomer and polymer and its adsorption of phenol and p-chlorophenol, Desal. Water Treat., 150 (2019) 192–203.
[33] K.Y. Foo, B.H. Hameed, Insights into the modeling of adsorption isotherm systems, Chem. Eng. J., 156 (2010) 2–10.
[34] E.S. Al-Allaq, H.S. Al-Lami, A.H. Al-Mowali, Synthesis and adsorption study of some chitosan acidic derivatives as dispersants for ceramic alumina powders, Egypt. J. Chem., 63 (2020) 2717–2736.
[35] A. Benhammou, A. Yaacoubi, L. Nibou, B. Tanouti, Adsorption of metal ions onto Moroccan stevensite: kinetic and isotherm studies, J. Colloid Interface Sci., 282 (2005) 320–326.
[36] M. Dubinin, The potential theory of adsorption of gases and vapors for adsorbents with energetically nonuniform surfaces, Chem. Rev., 60 (1960) 235–241.
[37] A. Debrassi, T. Baccarin, C.A. Demarchi, N. Nedelko, A. Ślawska-Waniewska, P. Dłużewski, M. Bilska, C.A. Rodrigues, Adsorption of Remazol red 198 onto magnetic N-lauryl

chitosan particles: equilibrium, kinetics, reuse and factorial design, Environ. Sci. Pollut. Res., 19 (2012) 1594–1604.
[38] A.-H. Chen, C.-Y. Yang, C.-Y. Chen, C.-Y. Chen, C.-W. Chen, The chemically crosslinked metal-complexed chitosans for comparative adsorptions of Cu(II), Zn(II), Ni(II) and Pb(II) ions in an aqueous medium, J. Hazard. Mater., 163 (2009) 1068–1075.
[39] A.-H. Chen, S.-M. Chen, Biosorption of azo dyes from aqueous solution by glutaraldehyde-crosslinked chitosans, J. Hazard. Mater., 172 (2009) 1111–1121.
[40] V.J. Inglezakis, A.A. Zorpas, Heat of adsorption, adsorption energy and activation energy in adsorption and ion exchange systems, Desal. Water Treat., 39 (2012) 149–157.
[41] H.T. Xing, J.H. Chen, X. Sun, Y.H. Huang, Z.B. Su, S.R. Hu, W. Weng, S.X. Li, H.X. Guo, W.B. Wu, NH_2-rich polymer/graphene oxide used as a novel adsorbent for removal of Cu(II) from aqueous solution, Chem. Eng. J., 263 (2015) 280–289.
[42] T. Manimekalai, G. Tamilarasan, N. Sivakumar, S. Periyasamy, Kinetic, equilibrium and thermodynamic studies of synthetic dye removal using plastic waste activated carbon prepared by CO_2 activation, Int. J. ChemTech. Res., 8 (2015) 225–240.
[43] A.M. Ghaedi, S. Karamipour, A. Vafaei, M.M. Baneshi, V. Kiarostami, Optimization and modeling of simultaneous ultrasound-assisted adsorption of ternary dyes using copper oxide nanoparticles immobilized on activated carbon using response surface methodology and artificial neural network, Ultrason. Sonochem., 51 (2019) 264–280.
[44] S. Patil, S. Renukdas, N. Patel, Removal of methylene blue, a basic dye from aqueous solutions by adsorption using teak tree (*Tectona grandis*) bark powder, Int. J. Environ. Sci. Technol., 1 (2011) 711–726.
[45] T. Egbosiuba, A. Abdulkareem, A. Kovo, E. Afolabi, J. Tijani, M. Auta, W. Roos, Ultrasonic enhanced adsorption of methylene blue onto the optimized surface area of activated carbon: adsorption isotherm, kinetics and thermodynamics, Chem. Eng. Res. Des., 153 (2020) 315–336.
[46] H. Erdem, B. Yildiz, M. Şahin, M. Erdem, Etodolac adsorption onto activated carbon prepared by chemical activation and pyrolysis of biomasses mixture, Biomass Convers. Biorefin., 10 (2020) 1153–1165.
[47] A. Itodo, H. Itodo, Activation chemistry and kinetics of Shea nutshell biosorbents for textile wastewater treatment, Acad. Arena, 2 (2010) 51–60.
[48] A.S. Özcan, B. Erdem, A. Özcan, Adsorption of Acid blue 193 from aqueous solutions onto BTMA-bentonite, Colloids Surf., A, 266 (2005) 73–81.
[49] C.H. Ko, C. Fan, P.N. Chiang, M.K. Wang, K.C. Lin, p-Nitrophenol, phenol and aniline sorption by organo-clays, J. Hazard. Mater., 149 (2007) 275–282.
[50] A. Gholizadeh, M. Kermani, M. Gholami, M. Farzadkia, Kinetic and isotherm studies of adsorption and biosorption processes in the removal of phenolic compounds from aqueous solutions: a comparative study, J. Environ. Health Sci. Eng., 11 (2013) 1–10.
[51] A.E. Regazzoni, Adsorption kinetics at solid/aqueous solution interfaces: on the boundaries of the pseudo-second-order rate equation, Colloids Surf., A, 585 (2020) 124093, doi: 10.1016/j.colsurfa.2019.124093.
[52] M.J. Rupa, A. Pal, B.B. Saha, Activated carbon-graphene nanoplatelets based green cooling system: adsorption kinetics, heat of adsorption, and thermodynamic performance, Energy, 193 (2020) 116774, doi: 10.1016/j.energy.2019.116774.
[53] S. Patil, J. Patil, S. Renukdas, N. Patel, Mechanism of adsorption of ferrous ions from waste water on natural adsorbents, World J. Pharm. Pharm. Sci., 4 (2015) 767–788.
[54] A. Harrou, E. Gharibi1, H. Nasri, M. El Ouahabi, Thermodynamics and kinetics of the removal of methylene blue from aqueous solution by raw kaolin, SN Appl. Sci., 2 (2020) 277–287.
[55] H.N. Tran, S.-J. You, H.-P. Chao, Thermodynamic parameters of cadmium adsorption onto orange peel calculated from various methods: a comparison study, J. Environ. Chem. Eng., 4 (2016) 2671–2682.
[56] O.A. Akinbulumo, O.J. Odejobi, E.L. Odekanle, Thermodynamics and adsorption study of the corrosion inhibition of mild steel by *Euphorbia heterophylla* L. extract in 1.5 M HCl, Results Mater., 5 (2020) 100074, doi: 10.1016/j.rinma.2020.100074.
[57] H. Ouassif, E.M. Moujahid, R. Lahkale, R. Sadik, F.Z. Bouragba, M. Diouri, Zinc-aluminum layered double hydroxide: high efficient removal by adsorption of tartrazine dye from aqueous solution, Surf. Interfaces, 18 (2020) 100401, doi: 10.1016/j.surfin.2019.100401.
[58] G.D. Vuković, A.D. Marinković, S.D. Škapin, M.Đ. Ristić, R. Aleksić, A.A. Perić-Grujić, P.S. Uskoković, Removal of lead from water by amino modified multi-walled carbon nanotubes, Chem. Eng. J., 173 (2011) 855–865.
[59] G.Z. Kyzas, N.K. Lazaridis, M. Kostoglou, Adsorption/desorption of a dye by a chitosan derivative: experiments and phenomenological modeling, Chem. Eng. J., 248 (2014) 327–336.
[60] O. Zanella, I.C. Tessaro, L.A. Féris, Desorption-and decomposition-based techniques for the regeneration of activated carbon, Chem. Eng. Technol., 37 (2014) 1447–1459.
[61] L. Soldatkina, M. Zavrichko, Equilibrium, kinetic, and thermodynamic studies of anionic dyes adsorption on corn stalks modified by cetylpyridinium bromide, Colloids Interfaces, 3 (2019) 1–13.
[62] A.A. Kamaru, N.S. Sani, N.A.N.N. Malek, Raw and surfactant-modified pineapple leaf as adsorbent for removal of methylene blue and methyl orange from aqueous solution, Desal. Water Treat., 57 (2016) 18836–18850.
[63] M. Vakili, S. Deng, G. Cagnetta, W. Wang, P. Meng, D. Liu, G. Yu, Regeneration of chitosan-based adsorbents used in heavy metal adsorption: a review, Sep. Purif. Technol., 224 (2019) 373–387.
[64] A. Abdulwahid, A.A. Alwattar, A. Haddad, M. Alshareef, J. Moore, S. Yeates, P. Quayle, An efficient reusable perylene hydrogel for removing some toxic dyes from contaminated water, Polym. Int., 70 (2021) 1–12.
[65] B. Priyadarshini, T.P. Tapas, R. Sahoo, An efficient and comparative adsorption of Congo red and Trypan blue dyes on MgO nanoparticles: kinetics, thermodynamics and isotherm studies, J. Magnesium Alloys, 9 (2021) 478–488.
[66] S. Al-Salihi, A.M. Jasim, M.M. Fidalgo, Y. Xing, Removal of Congo red dyes from aqueous solutions by porous γ-alumina nanoshells, Chemosphere, 286 (2022) 131769, doi: 10.1016/j.chemosphere.2021.131769.
[67] M.A. Farghalia, A.M. Selimb, H.F. Khaterc, N. Bagatod, W. Alharbie, K.H. Alharbie, I.T. Radwanf, Optimized adsorption and effective disposal of Congo red dye from wastewater: hydrothermal fabrication of MgAl-LDH nanohydrotalcite-like materials, Arabian J. Chem., 15 (2022) 104171, doi: 10.1016/j.arabjc.2022.104171.